Available online at www.sciencedirect.com
SCIENCE DIRECT®
Journal of Power Sources 147 (2005) 32–45
JOURNAL OF POWER SOURCES
www.elsevier.com/locate/jpowsour

Review

Mathematical modeling of polymer electrolyte fuel cells

Ruy Sousa Jr, Ernesto R. Gonzalez *

Departamento de Físico-Química do Instituto de Química de São Carlos, Universidade de São Paulo, Av. Trabalhador Sãocarlense 400, Caixa Postal 780, 13560-970 São Carlos SP, Brazil

Received 25 January 2005; accepted 11 March 2005
Available online 9 June 2005

Abstract

Fuel cells with a polymer electrolyte membrane have been receiving more and more attention. Modeling plays an important role in the development of fuel cells. In this paper, the state-of-the-art regarding modeling of fuel cells with a polymer electrolyte membrane is reviewed. Modeling has allowed detailed studies concerning the development of these cells, e.g. in discussing the electrocatalysis of the reactions and the design of water-management schemes to cope with membrane dehydration. Two-dimensional models have been used to represent reality, but three-dimensional models can cope with some important additional aspects. Consideration of two-phase transport in the air cathode of a proton exchange membrane fuel cell seems to be very appropriate.

Most fuel cells use hydrogen as a fuel. Besides safety concerns, there are problems associated with production, storage and distribution of this fuel. Methanol, as a liquid fuel, can be the solution to these problems and direct methanol fuel cells (DMFCs) are attractive for several applications. Mass transport is a factor that may limit the performance of the cell. Adsorption steps may be coupled to Tafel kinetics to describe methanol oxidation and methanol crossover must also be taken into account. Extending the two-phase approach to the DMFC modeling is a recent, important point.

Keywords: Fuel cell; Polymer electrolyte membrane; Methanol feed; Mathematical modeling; Review

Contents

1. Introduction

Modeling plays an important role in the development of fuel cells, because it allows a better comprehension of the parameters affecting the performance of single fuel cells and fuel cell systems [1].

Fuel cells with a polymer electrolyte membrane have been receiving more and more attention. The main characteristics of this kind of fuel cell are the operation without the generation of pollutants, less corrosion problems, high power density and low temperature start-up. However, there are several problems to be solved, such as mem-

* Corresponding author. Tel.: +55 16 33739899; fax: +55 16 33739952.
E-mail address: ernesto@iqsc.usp.br (E.R. Gonzalez).

0378-7753/$ – see front matter © 2005 Elsevier B.V. All rights reserved.
doi:10.1016/j.jpowsour.2005.03.191

Nomenclature

a	effective catalyst area per volume (cm^{-1})
a_{ht}	heat transfer area per unit length (cm)
b	Tafel slope (V)
b_{cell}	parameter ($V\,dec^{-1}$)
c_a	dimensionless capacitance for the agglomerate network
$c_F^{CH_3OH}$	methanol feed concentration ($mol\,dm^{-3}$)
c_f	concentration of membrane fixed-charge-site species ($mol\,cm^{-3}$)
c_k	molar concentration of k ($mol\,cm^{-3}$)
c_w	concentration of water in the membrane ($mol\,cm^{-3}$)
C_{dl}	double layer capacitance (F)
C_1	parameter (V)
C_2	parameter ($cm^2\,A^{-1}$)
d	channel height (cm)
D_k^{eff}	effective mass diffusivity ($cm^2\,s^{-1}$)
D_λ	corrected diffusion coefficient ($cm^2\,s^{-1}$)
D_{ij}	diffusion coefficient ($cm^2\,s^{-1}$)
E^0	parameter (V)
E_0^*	parameter (V)
f	frequency (rpm)
F	molar flow rate of methanol ($mol\,s^{-1}$)
F_T	total molar flow rate of gas ($mol\,m^{-1}\,s^{-1}$)
h	channel width (cm)
h_a	height of the active catalyst layer (m)
h_f	height of the flow channel (m)
h_p	height of the porous backing (m)
h_t	heat transfer coefficient ($W\,m^{-2}\,K^{-1}$)
H_{cm}	location of cathode catalyst layer (cm)
ΔH	enthalpy gradiente ($J\,mol^{-1}$)
i	current density ($A\,cm^{-2}$)
i_d	limiting current density ($A\,cm^{-2}$)
i_0	exchange current density ($A\,cm^{-2}$)
I	current density ($A\,cm^{-2}$)
I_l	current density at the limiting current density ($A\,cm^{-2}$)
$I_L^{O_2}$	limiting current density due to limiting oxygen diffusion ($A\,cm^{-2}$)
I_p	parasitic current density at cathode ($A\,cm^{-2}$)
j	$(-1)^{1/2}$
j^{MeOH}	methanol mass flux ($kg\,cm^{-2}\,s^{-1}$)
j_0	exchange current density referenced to pure oxygen at 1 atm ($A\,cm^{-2}\,atm^{-1}$)
J	current density ($A\,cm^{-2}$)
k_p	hydraulic permeability (cm^2)
k_ϕ	electrokinetic permeability (cm^2)
L	cell channel length (cm)
m_{H^+}	molality of H^+ ($mol\,g^{-1}$)
M_m	equivalent weigh of membrane
M_i	molar flow rate of i ($mol\,s^{-1}$)
M^{MeOH}	molecular weight of methanol ($kg\,mol^{-1}$)
$dM_{w,k}^l/dx$	water condensation or evaporation ($mol\,cm^{-1}\,s^{-1}$)
n_{drag}	electro-osmotic drag coefficient
$N_{i,y,k}$	molar flux of i in k channel ($mol\,cm^{-2}\,s^{-1}$)
N_i	molar flux of i ($mol\,cm^{-2}\,s^{-1}$)
N_w	water molar flux ($mol\,cm^{-2}\,s^{-1}$)
$N_{w,c}$	water molar flux produced at cathode ($mol\,cm^{-2}\,s^{-1}$)
p	hydraulic pressure (atm)
P	pressure (atm or Pa)
P_C	critical pressure (atm)
P_w	partial pressure of water in the membrane (atm)
R	resistance ($\Omega\,cm^2$)
R_{lf}	low frequency resistance (Ω)
R_m	membrane resistance ($\Omega\,cm^2$)
R_s	solution resistance (Ω)
R_1	dimensionless resistance in the agglomerate network
s	liquid water saturation
SH	cell height (cm)
SW	cell width (cm)
S	flooding parameter
S_u	momentum source term ($kg\,cm^{-3}\,s^{-2}$)
S_k	species source term ($mol\,cm^{-3}\,s^{-1}$)
S_ϕ	potential source term ($S\,V\,cm^{-3}$)
t_m	membrane thickness (cm)
t_A	anode thickness (cm)
t_C	cathode thickness (cm)
T	temperature (°C or K)
T_a	temperature of the anode stream (°C)
T_c	temperature of the cathode stream (°C)
T_s	temperature of the solid phase (°C)
$\vec{u}$	velocity vector ($cm\,s^{-1}$)
U_{ht}	overall heat transfer coefficient ($J\,s^{-1}\,cm^{-2}\,°C^{-1}$)
U_s	(1 + S/M) (where S/M is the molar ratio of steam to methanol)
v	velocity ($cm\,s^{-1}$)
V_{cell}, U_{cell}, E	cell potential (V)
V_{oc}	open cell potential (V)
W	weight of catalyst (kg)
x	distance (cm or m)
x_i	mole fraction of i
$x_{o,c}$	mole fraction of oxygen at cathode
x_{liq}	mole fraction of liquid water
x_{met}	conversion ratio of methanol
y	distance (cm or m)
Y_s	$U(r_1(0) + r_2(0))$ ($mol\,kg^{-1}\,s^{-1}$)
z	distance (cm or m)
z_{H^+}	charge number of H^+
z_f	charge number of membrane fixed-charge-site species
Z	impedance in the electrolyte (Ω)

$Z_{electrode}$ total impedance (Ω)
Z_s $(Ur_1(0) - 2r_2(0))$ (mol kg^{-1} s^{-1})

Greek letters
α_a anodic transfer coefficient
α_c cathodic transfer coefficient
ε porosity
$\varepsilon_g^{d^+}$ cathode gas porosity
ϕ potential (V)
Φ dc potential-independent agglomerate diffusion parameter
Γ thin film diffusion parameter
η overpotential (V)
λ water content in the membrane
μ viscosity (g cm^{-1} s^{-1})
μ_c empirical constant
μ^{eff} effective viscosity (kg m^{-1} s^{-1})
μ_{H^+} chemical potential of H^+ (J mol^{-1})
μ_r reduced overpotential
ρ density (kg cm^{-3})
ρ_{dry} density (g cm^{-3})
σ^{eff} effective ionic conductivity (S cm^{-1})
σ_m membrane conductivity (Ω^{-1} cm^{-1})
ϖ angular frequency (rad s^{-1})
ϖ_a characteristic agglomerate frequency (rad s^{-1})
ϖ_f characteristic thin film frequency (rad s^{-1})
Ψ ac potential-dependent agglomerate diffusion parameter
ζ stoichiometric flow ratio (amount of reactant in the chamber feed divided by the amount required by the electrochemical reaction) based on the reference current density of 1 A cm^{-2}.

brane dehydration, because of the water transport in the fuel cell, the high catalyst cost [2] and the poisonous effect of contaminants.

The optimal modeling approach differs for each application. It is important to define, initially, the area of interest of the model. It can be at the fundamental cell level, including the inlet channels, the electrodes and the membrane, on a higher level where individual fuel cells are gathered in a stack, or on the complete system level consisting of a fuel cell stack with its compressor, pumps, humidifiers, etc. [1]. In Haraldsson and Wipke [1], the analysis is directed to the evaluation of fuel cell system models. In this review, we will mainly be concerned with modeling at the fundamental cell level.

A mechanistic fuel cell model is based on transport phenomena and electrochemical relationships. On the other hand, there are empirical models, developed specifically for each application and set of operating conditions (such as in Kim et al. [3] and Squadrito et al. [4]). There are still, semi-empirical models in which the introduction of some phenomenological knowledge into empirical relations can improve the predictability of the empirical model. When a tool for detailed studies is desired, as many as possible mechanistic theoretical considerations must be taken into account.

The operating regime associated with the model can be either steady-state or transient. Defining spatial dimension and complexity is also important. Validation, in turn, is important to guarantee that the model is a useful and reliable tool.

2. Fuel cell modeling

Springer and Raistrick [5] took into account, in the modeling of a porous electrode with oxygen diffusion, the "flooded-agglomerate" approach of Giner and Hunter [6] coupled to a thin-film diffusion process. The electrode structure was considered to be a macro-microporous interconnected system, with hydrophobic regions allowing reactant gas access to the surface of agglomerate regions. The agglomerate consists of regions of catalyst containing carbon and electrolyte, and is separated from the hydrophobic gas regions by a thin film of electrolyte. Reactant gas can dissolve in the electrolyte and diffuse to the catalyst sites. Transfer functions developed allow a combination of a simplified agglomerate representation with the thin film element, facilitating numerical fitting of the model to measured impedance data. Perez et al. [7] used Springer and Raistrick approach (for simulation and analysis of dc and ac polarization results) in studies on the electrocatalysis of the oxygen reduction reaction on platinum on carbon thin porous coating rotating disk electrode (TPC/RDE). The TPC/RDE is an experimental apparatus conceptually similar to a flooded-agglomerate, given by the electrode structure, in contact with a thin film of thickness determined by the rotation rate of the electrode. Steady-state polarization (fitted using Eq. (1a)) and the impedance (fitted using Eq. (1b)) results showed a duplication of the Tafel slope (Fig. 1a) in alkaline medium (in acid medium, there is a duplication first and then a quadruplication, Fig. 1b). The duplication in alkaline medium and the first duplication in acid medium are due to structural effects in the catalyst layer of the electrode [7]:

$$\frac{i}{i_0} = \frac{\exp\mu_r(\tanh[\Phi\exp(\mu_r/2)])/[\Phi\exp(\mu_r/2)]}{1+\Gamma\exp\mu_r(\tanh[\Phi\exp(\mu_r/2)])/[\Phi\exp(\mu_r/2)]} \quad (1a)$$

$$\begin{aligned} Z &= \{\exp\mu_r(i_0/b)/(1+\Gamma\exp\mu_r/R_l) \\ &\times[1/(R_1+(1/((1/(((1/2)(\mathrm{sech}^2\Phi\exp(\mu_r/2)) \\ &+(1/R_1))^{-1}-R_1))+jc_a(\varpi/\varpi_a)))) \\ &-((\Gamma\exp\mu_r/R_1)(1+(\Phi^4\exp(2\mu_r)/16))^{1/4} \\ &\times(\tanh\Psi/\Psi)^2(\tanh\sqrt{j(\varpi/\varpi_f)}/\sqrt{j(\varpi/\varpi_f)}))/ \\ &(1+\Gamma\exp\mu_r(\Psi^2/(\Phi^2\exp\mu_r))(\tanh\Psi/\Psi) \\ &(\tanh\sqrt{j(\varpi/\varpi_f)}/\sqrt{j(\varpi/\varpi_f)}))]\}^{-1} \end{aligned} \quad (1b)$$

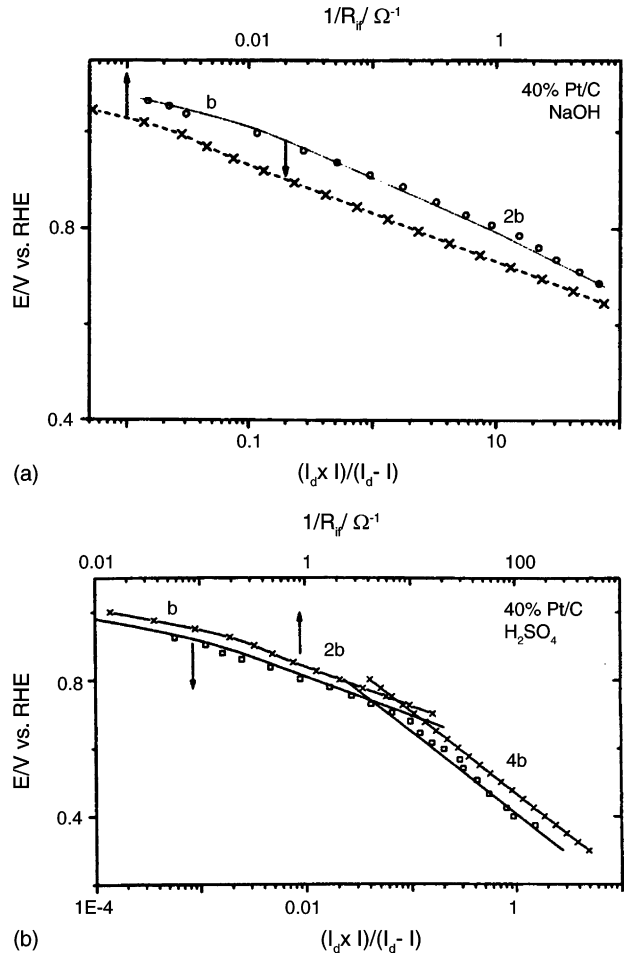

Fig. 1. (a) Mass-transport corrected Tafel plots for oxygen reduction on 40% Pt/C in 1.0 M NaOH. (×) $\log(1/R_{lf})$ vs. E; (●) $\log[(I_d \times I)/(I_d - I)]$ vs. E; (full line) fitted plot using Eq. (1a) with $\Gamma \to 0$. $f = 2500$ rpm (reprinted from [7], Copyright 1998, with permission from Elsevier Science). (b) Mass-transport corrected Tafel plots for oxygen reduction on 40% Pt/C in 0.5 M H_2SO_4. (×) $\log(1/R_{lf})$ vs. E; (●) $\log[(I_d \times I)/(I_d - I)]$ vs. E; (full line) fitted plot using Eq. (1a) with $\Gamma \to 0$. $f = 2500$ rpm (reprinted from [7], Copyright 1998, with permission from Elsevier Science).

In Springer et al. [8], the distribution of water in a polymer electrolyte fuel cell is calculated by considering the water flow through two inlet channels, two gas-diffusion electrodes and a Nafion membrane (Fig. 2).

Water enters the fuel cell assembly as a component of the humidified fuel and oxidant streams, and by generation associated with the cell reaction. Diffusion of water vapor and hydrogen occurs through the anode, while ternary diffusion of water vapor, oxygen and nitrogen occurs through the cathode. These diffusion processes through the porous electrodes are calculated starting from the Stefan–Maxwell equation (Eq. (2)):

$$\frac{\mathrm{d}x_i}{\mathrm{d}z} = RT \sum_j \left(\frac{x_i N_j - x_j N_i}{P D_{ij}} \right) \tag{2}$$

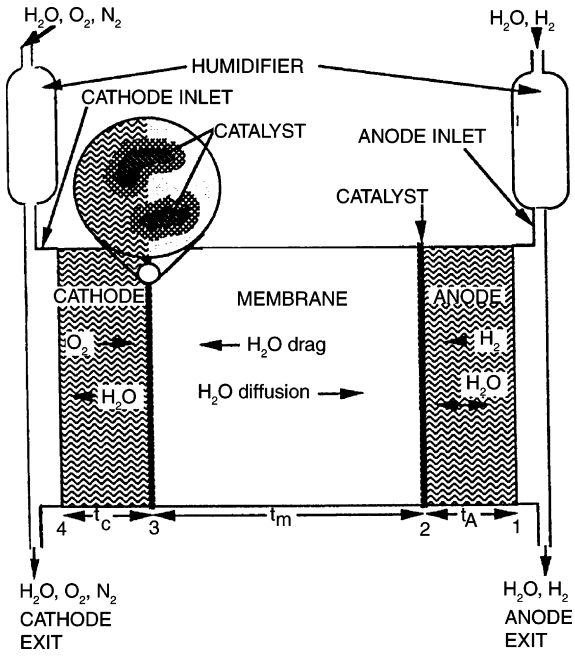

Fig. 2. Schematic diagram of fuel cell model (reprinted from [8], Copyright 1991, reproduced by permission of The Electrochemical Society, Inc.).

Equilibrium of water is assumed at the electrode/membrane interface. The net flux of water through the membrane considers the electro-osmotic and the diffusion driving forces for water ($N_w = n_{drag}(2N_{w,c})(\lambda/22) - (\rho_{dry}/M_m)D_\lambda(\mathrm{d}\lambda/\mathrm{d}z)$). When the material balances are solved, the membrane resistance $R_m = \int_0^{t_m}(1/\sigma(\lambda))\,\mathrm{d}z$, the O_2 concentration at the catalyst interface and the cathode overpotential (by using the Tafel expression $J = j_0 P_C(x_{o,c}/(1 - x_{liq}))\exp[0.5F\eta/(R_g T)]$) are determined. So, a potential versus current curve for the fuel cell can be determined ($V_{cell} = V_{oc} - \eta - JR_m$). The active catalyst layer is assumed to exist as a thin plane at the electrode/membrane interface (as it is considered in the majority of the complete cell models); the rest of the electrode serves only as a gas diffusion region. The Springer et al. model predicted the increase in membrane resistance with increased current density and pointed out the advantage of thinner membranes in reducing this problem.

In Bernardi and Verbrugge [9], a similar modeling of a polymer electrolyte fuel cell is presented. The cell consists of a membrane sandwiched between two gas-diffusion electrodes (membrane and electrodes assembly, MEA), hot pressed and placed between two current collectors. Humidified gaseous H_2 enters the anode gas chamber, is transported through the porous gas diffusion layer and dissolves in the electrolyte phase at the anode catalyst layer where it is oxidized. The gaseous reactant O_2, mixed with nitrogen and water vapor, enters into the cathode gas chamber, is transported through the porous gas diffusion layer and dissolves in the electrolyte phase at the cathode catalyst layer. Protons transported through the membrane participate in the reduction of the dissolved O_2 at catalyst sites. Bernardi and Verbrugge assume that the system operates at constant tem-

perature. It is also assumed steady-state operation. They consider a fully hydrated membrane and wet pores in the gas diffusion layer (assuming no interactions between liquid and gas flows). The equations constituting the mathematical model of the cell are derived from basic phenomenological relationships (such as a form of Schlögl's velocity equation (Eq. (3a)), the Butler–Volmer equation for charge transfer (Eq. (3b)) and the Stefan–Maxwell equation for gas-phase transport):

$$v = \left(\frac{k_\phi}{\mu}\right) z_f c_f F \left(\frac{d\phi}{dz}\right) - \left(\frac{k_p}{\mu}\right)\left(\frac{dp}{dz}\right) \quad (3a)$$

$$J = i_0 \left\{ \exp\left[\alpha_a \left(\frac{F}{R_g T}\right)\eta\right] - \exp\left[-\alpha_c \left(\frac{F}{(R_g T)}\right)\eta\right]\right\} \quad (3b)$$

These, along with appropriate conservation principles of physics allow deriving the coupled differential equations for the cell model. The necessary parameters and properties were appropriately considered and estimated. For the base-case, results do not show cell polarization resulting from limitation on the transport of O_2 (Fig. 3a). However, by decreasing the cathode gas porosity, the limited transport of oxygen through the cathode diffusion layer to the reaction sites may increase the cathode overpotential (Fig. 3b).

It also showed that membrane dehydration could cause limitations on the operating current density. In this case, efficient water-management schemes are necessary.

In 1993, Fuller and Newman published a paper [10] in which it is considered a fuel cell operating in a steady-state regime on air and reformed methanol. The transport of species in the polymer electrolyte was described by a fundamental equation that may be put in the form of the Stefan–Maxwell equation and combined with the appropriate material balance of each species. The Stefan–Maxwell equations could also be used to describe multicomponent diffusion of gases. Electron-transfer reactions were described by Butler–Volmer kinetics. The energy released by the overall chemical reaction was split into electrical work, change in the enthalpy (and hence in the temperature) of the flowing gas streams and external heat transfer (Eq. (4)). Heat removal is also important in the fuel cell operation:

$$\int_0^z h_t(T - T_{Ambient})\,dz + \int_0^z V_{cell} I\,dz + F_T \Delta H = 0 \quad (4)$$

In 1993, Nguyen and White were also concerned with the water and heat management in proton exchange membrane fuel cells, which are essential features for obtaining high power densities. A water and heat management model was developed [11] and used to investigate the effectiveness of different humidification designs. The model is a steady-state, two-dimensional one. The model regions (Fig. 4) consist of flow channels on both sides of the membrane/electrode (one

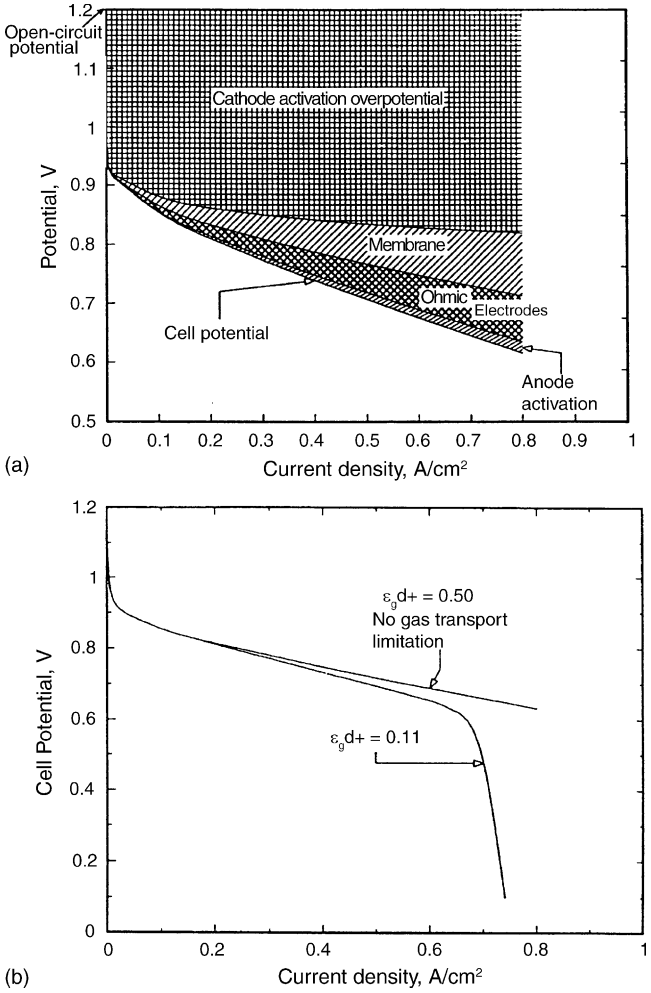

Fig. 3. (a) Model calculations of the contributions to fuel cell potential losses as a function of operating current density for base case conditions (reprinted from [9], Copyright 1992, reproduced by permission of The Electrochemical Society, Inc.). (b) Model calculations of the fuel cell potential as a function of operating current density for two values of cathode gas porosity $\varepsilon_g^{d^+}$ (reprinted from [9], Copyright 1992, reproduced by permission of The Electrochemical Society, Inc.).

system for the oxygen cathode and another one for the hydrogen anode).

The model takes into account mass transport of water and gaseous reactants across the membrane/electrode and along the flow channels and heat transfer between the solid phases and the gases along the flow channels. The change in the number of moles (quantified by the material balances) of a single-phase species along the channel length is due to the normal flux into or out of the membrane/electrode ($dM_i/dx = hN_{i,y,k}$). For water, the material balance also takes into account the possibility of condensation or evaporation (quantified by the term ($dM^l_{w,k}/dx$)). It is assumed that water leaves the channel and enters the electrode in the form of vapor only. Liquid water is assumed to exist in the form of small droplets with negligible volume. The electrodes are considered ultrathin (gas diffusion through the electrode

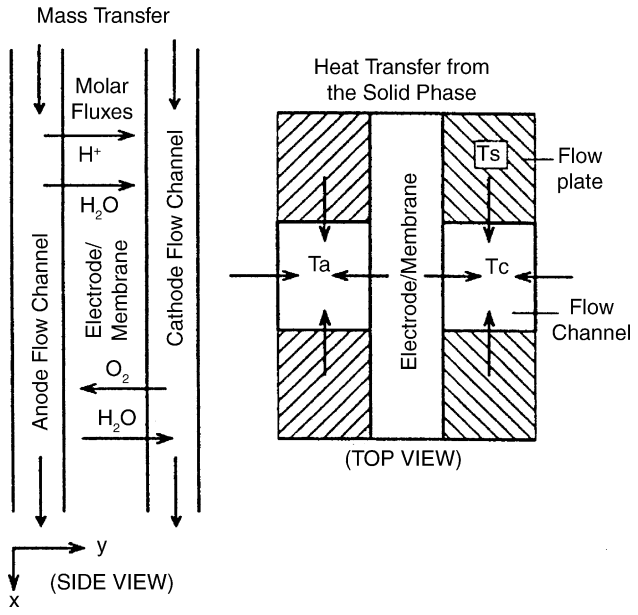

Fig. 4. Schematic of modeled regions (reprinted from [11], Copyright 1993, reproduced by permission of The Electrochemical Society, Inc.).

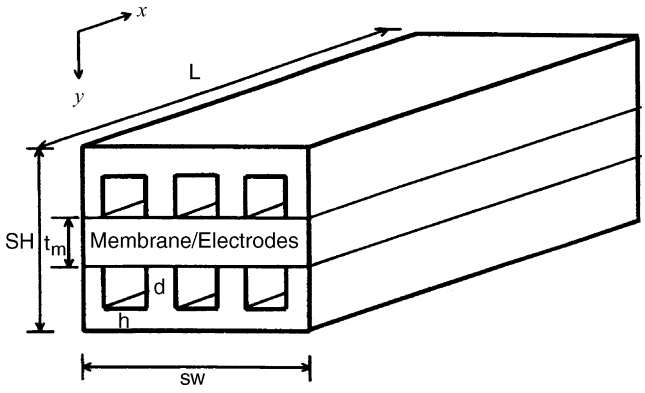

Fig. 5. Schematic diagram of modeling region (reprinted from [12], Copyright 1998, reproduced by permission of The Electrochemical Society, Inc.).

porous layer is neglected). The molar flux of each component is proportional (depending on the stoichiometry of the electrochemical reactions) to the local current density, which varies along the channel length as the membrane conductivity and the overpotential of the electrodes change. The net water flow in the membrane is associated to migration (water molecules carried by protons) and diffusion effects. Adequate expressions to estimate important parameters, such as the water diffusion coefficient and the electro-osmotic drag coefficient, were used. The energy balance equation for the anode and cathode gaseous streams takes into account water condensation and evaporation (proportional to $dM^{l}_{w,k}/dx$) in the flow channel and heat transfer due to the temperature gradient between the solid phase and the interior of the channels. The cell potential is calculated accounting for the membrane resistance and the electrode polarizations. Modeling results showed that at high current densities, the back diffusion of water from the cathode side of the membrane is insufficient to keep the membrane hydrated. Water injection into the anode flow channel can improve the cell performance for supplying the humidification to maintain the anode hydrated, and also for contributing to the heat removal. When air is used (instead of pure oxygen), the cathode stream must also be humidified.

In the previously cited Nguyen and White's work [11], the temperature of the solid phase (flow channel plates, electrodes and membrane) was considered uniform and constant. In practice, a temperature gradient in the solid layers along the flow channels of the fuel cell may exist (the term $U_{ht}a_{ht}(T_{solid} - T_{channel})$ accounts for the energy transported from the fluid to the solid layer), and this gradient can affect the temperature distribution of the fluid in the flow channels and also the hydration state of the membrane along the flow path. To better deal with these problems, a new model was developed [12], based on Nguyen and White [11], to describe the temperature distribution in the solid phase along the flow path of the anode and cathode faces of the fuel cell (Fig. 5).

The model was extended to include the convective water transport across the membrane by a pressure gradient (quantified by the term $c_w(k_p/\mu)(dP_w/dy)$) and the heat removal by heat exchangers. A pressure gradient between the cathode and anode can increase the water back transport across the membrane (although it can be demonstrated that the fuel cell pressurization involves an energy cost that hardly compensates the gain in performance—De Souza and Gonzalez [13]), while using appropriate heat exchangers can be amply effective for heat removal and distribution. Dannenberg et al. [14] presented a modeling work according to an approach very similar to those of the previously cited Nguyen and collaborators' works.

In the work of Sena et al. [15], a simplified model is used to describe the water transport in a polymer electrolyte membrane of a H_2–O_2 fuel cell operating at low temperatures; a diffusion mechanism is considered for water back transport. Combined with the Tafel equation, it led to an analytical expression for the description of the cell potential as a function of the current density. Additionally, limiting effects due to oxygen diffusion were included (Eq. (5)):

$$E = E^0 - b\log I + b\log\left(1 - \left(\frac{I}{I_L^{O_2}}\right)\right) - RI \qquad (5)$$

Results showed that for Nafion 115 and 117 membranes, water transport through the membrane is a limiting factor. For Nafion 112, on the other hand, oxygen diffusion effects (in the gas diffusion electrode) dominate the potential–current relationship.

In Gurau et al. [16], a two-dimensional model for the entire sandwich of a H_2–O_2 proton exchange membrane fuel cell was developed. Standard momentum, energy transport, continuity and species concentration equations were solved in the gas channels, while the porous media model was used for the equations describing transport phenomena in the membrane and the gas diffusion electrodes (in particular, with

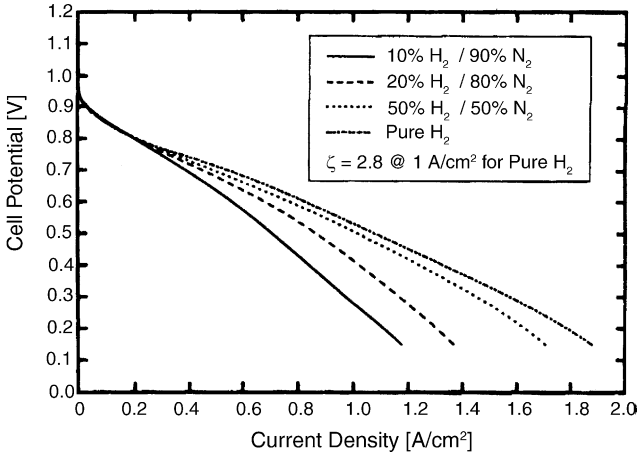

Fig. 6. Effect of the inlet hydrogen mole fraction on cell polarization curves (reprinted from [17], Copyright 2000, reproduced by permission of The Electrochemical Society, Inc.).

the velocity field provided by a generalized form of Darcy's law, obtained from the standard Navier–Stokes equations). By solving the transport equations, as well as relationships for the electrochemical reactions, polarization curves under various operating conditions were obtained. In contrast to the approach of Gurau et al., which used separate differential equations for different subregions, Um et al. [17] considered a single-domain approach, in which a single set of equations valid for all subregions is used. The fuel cell operation considering isothermal conditions is described by conservation principles of mass, momentum, species and charge (Eqs. (6a)–(6d)):

$$\frac{\partial(\varepsilon\rho)}{\partial t} = -\nabla\cdot(\varepsilon\rho\vec{u}) \tag{6a}$$

$$\frac{\partial(\varepsilon\rho\vec{u})}{\partial t} = -\nabla\cdot(\varepsilon\rho\vec{u}\vec{u}) - \varepsilon\nabla P + \nabla\cdot(\varepsilon\mu^{\mathrm{eff}}\nabla\vec{u}) + S_{\mathrm{u}} \tag{6b}$$

$$\frac{\partial(\varepsilon c_k)}{\partial t} = -\nabla\cdot(\varepsilon\vec{u}c_k) + \nabla\cdot(D_k^{\mathrm{eff}}\nabla c_k) + S_k \tag{6c}$$

$$0 = \nabla\cdot(\sigma^{\mathrm{eff}}\nabla\phi) + S_\Phi \tag{6d}$$

The momentum source term is used to describe Darcy's drag for flow through the porous electrodes and the membrane. The species and potential source terms, in their turn, are related to generation (or consumption) of species and the creation of electric current (kinetic expressions were derived from the Butler–Volmer equation). The boundary conditions are required only at the external surfaces of the spatial domain due to the single-domain approach used. The conservation equations were discretized and solved by using a general-purpose CFD (computational fluid dynamics) algorithm. The model could show (Fig. 6) that in the presence of hydrogen dilution in the fuel stream, hydrogen is depleted at the reaction surface, resulting in substantial anode mass transport polarization (this study can be of interest when considering reformed gas as the anode feed).

In a subsequent work, Um and Wang [18] present a three-dimensional model (Fig. 7) to cope with some additional aspects, such as the study of a mass-transport limitation not discussed in Um et al. [17], the rib effect. The two-dimensional simulation overpredicts the current density, because the landing area obstructing the gas transport is neglected [18]. The design of an innovative flow field, called interdigitated, was also studied. Yi and Nguyen [19] attempted to develop a two-dimensional model for this flow field. De Souza and Gonzalez [13] demonstrated experimentally the advantages of the interdigitated flow field. In this flow field, the reactant gas is forced by convection to pass through the porous gas diffusion layer in order to leave the system (inlet and outlet channels are not connected).

This forced convection mechanism facilitates the transport of reactants and products. Two-dimensional models are limited in their capability to represent the three-dimensional nature of the interdigitated flow. The three-dimensional simulations are again based on a single-domain fuel cell model. The model consists of non-linear, coupled partial differential equations representing the conservation of mass, momentum, species and charge with electrochemical reactions. Again, the conservation equations were discretized and solved by using a general-purpose CFD algorithm.

In Dutta et al. [20], two-phase transport is also neglected. In Janssen [21], a two-phase water transport model is presented, but it results in equations that are difficult to implement in a general purpose CFD algorithm. In Wang et al. [22], the so-called Multiphase Mixture Model [23,24] is applied to study the two-phase water transport in the porous air cathode of a proton exchange membrane fuel cell. Water condensation in the porous cathode is a usual phenomenon at high current densities. As the current density (and the water generation) increases, water is present first as vapor only. When the water vapor density at the membrane/cathode interface reaches the saturation value corresponding to the operating temperature, liquid water begins to appear. With further increase in the current density, the two-phase zone expands and its front propagates towards the flow channel (Fig. 8).

In the mixture approach [23,24], the differential balances are applied to a phase mixture (and appropriate additional algebraic relationships allow to obtain information on each single phase). The momentum balance equation reduces to an extended Darcy's law for two phase flow in porous media. The equation for the transport of species is applicable to oxygen as well as water. The mixture model is mathematically equivalent to the standard two-phase model used in a large number of applications of transport in porous media, such as petroleum exploitation problems; however, the mixture model is easier to implement [23,24]. In Wang et al. [22], the cell temperature was considered constant, and the model isothermal (however, an energy equation may improve the analysis—Berning et al. [25]). Inside the two-phase zone, the transport of liquid water is controlled by capillary action.

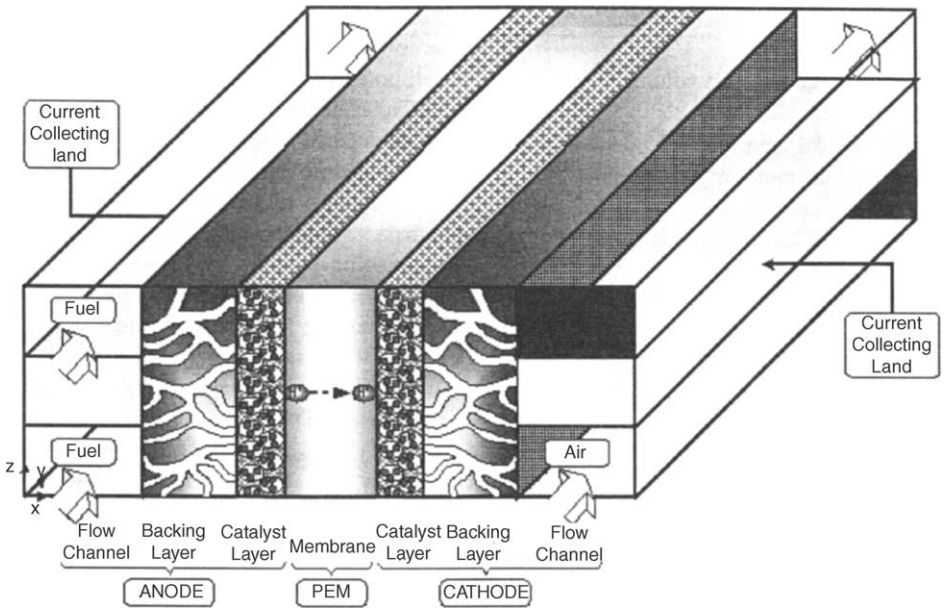

Fig. 7. Three-dimensional schematic diagram (reprinted from [18], Copyright 2004, with permission from Elsevier Science). Straight and interdigitated flows are studied by changing the flow inlet and outlet locations.

In Pisani et al. [26], a semi-empirical model is presented, which predicts the cell-potential versus current density (Eq. (7)). The derivation had the objective of characterizing the largest number of mechanism-based fitting coefficients, instead of purely empirical ones (such as in Kim et al. [3] and Squadrito et al. [4]). It was based on the fact that the main non-linear contributions to the cell potential drop in H_2–air fuel cells arise in the cathode:

$$V_{\text{cell}} = E^0 - RI - b\ln(I) + a\ln\left(1 - \left(\frac{I}{I_1}\right) S^{-\mu_c(1-(I/I_1))}\right) \quad (7)$$

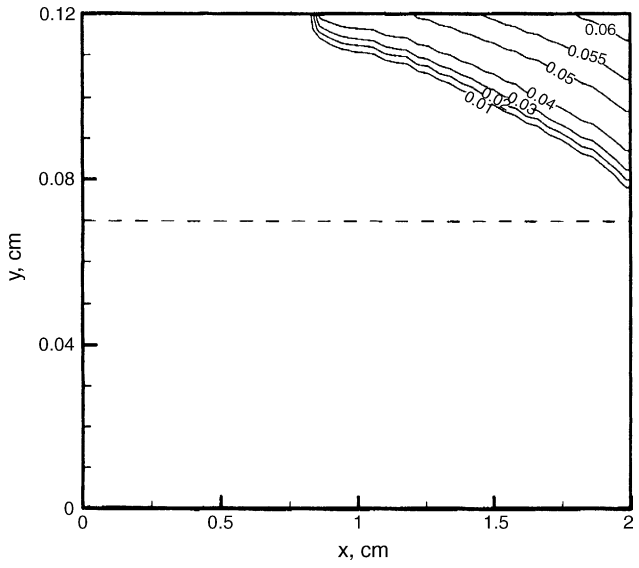

Fig. 8. Liquid water saturation contours in the porous cathode and flow channel at the current density of 1.4 A cm^{-2}. The evaporation front separating the two-phase zone from the single-phase region is approximately represented by the contour of $s = 0.01$ (reprinted from [22], Copyright 2001, with permission from Elsevier Science). $y < 0.07$ cm, flow channel; $y > 0.07$ cm, porous cathode.

In Mazumder and Cole [27], a three-dimensional model is presented, which carefully extracts the good elements from the existing models in the area. In some aspects, changes and improvements were made. The modeling is based on the solution of conservation equations. Electrochemical reactions inside the porous electrodes are described by using Butler–Volmer equations. The catalyst layer is treated as a finite sized region rather than a thin plane or a boundary. The resistance to the diffusion of the gaseous species imposed by the electrolyte (at the catalyst) is quantified by using an effective diffusion coefficient and considering that the overall porosity of the active catalyst layer is smaller than that of the gas diffusion layer. The model is non-isothermal. There are some fundamental points in the modeling.

Porous media transport

Conservation equations of momentum and mass in a porous media: The momentum equation is of the type of a Darcy's equation.

Conservation equation for energy: Electrical work, Joule heating and energy interactions because of phase changes are considered, besides the irreversible reaction losses due to the conversion of chemical energy into heat.

Species conservation: The transport of species in gaseous regions is quantified by using the Stefan–Maxwell equations.

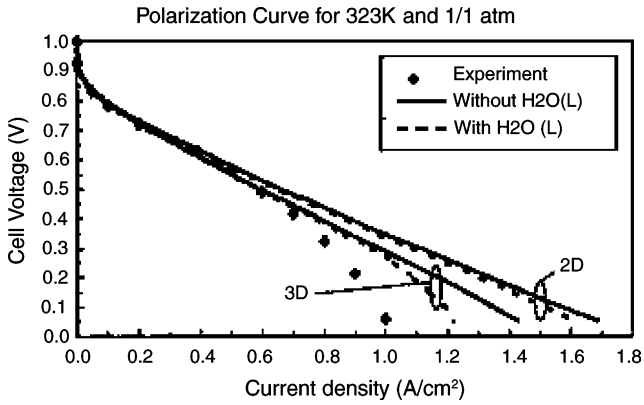

Fig. 9. Comparison of experimentally measured performance [29,30] with numerical predictions with and without liquid water formation and transport (reprinted from [28], Copyright 2003, reproduced by permission of The Electrochemical Society, Inc.).

Electrochemical reactions and coupling to mass and current transport

Electrochemical reactions occur at the interface of the catalyst clusters and the polymer electrolyte. It is where the gas comes in contact with the catalyst clusters and at these points, the diffusion flow is exactly balanced by the reaction flow. The charge transfer current density is obtained from the Butler–Volmer equation.

The solution of the set of conservation equations was performed within the framework of a commercial CFD code.

In Mazumder and Cole [28], formation and transport of liquid water in the proton exchange membrane fuel cell is included. The model is based on the multiphase mixture model (such as in Wang et al. [22]). The model base is an additional equation for the formation and transport of liquid water. Such equation includes mainly transport associated with electro-osmotic drag, influence of surface tension, phase change (condensation or evaporation). Liquid water can also reduce the diffusivity of the gaseous species. The "real" porosity for the gas phase species is called wet porosity (and is a function of the liquid saturation of the pore, which is defined as the volume fraction of the total pore space occupied by the liquid). The inclusion of liquid water formation and transport improved the predictive capability of the model (Fig. 9).

Knudsen diffusion (which occurs when the pores are very tiny) was neglected, and it is worth mentioning that Wohr et al. [31] are one of the few that attempted to take into account Knudsen-diffusion when considering the diffusion layer of an electrode, but no discussion is presented.

Additional references regarding modeling of proton exchange membrane fuel cells are: Eikerling and Kornyshev [32] (in which a homogeneous model for the cathode is considered); Kulikovsky et al. [33] (in which some local features generated by geometric aspects, e.g. the low concentrations of reactants in front of current collectors, are studied); Mann et al. [34] (in which an interesting feature of the model is a term to account for membrane ageing); Maggio et al. [35] (in which simulation results allow a comparison of different membranes); Rowe and Li [36] (in which a model is developed to study thermal effects); Ge and Yi [37] (in which a model is used to compare counterflow mode to coflow regime); Yerramalla et al. [38] (in which a fuel cell stack system is also simulated).

Most of the fuel cells use hydrogen as a fuel. Besides safety concerns, there are problems associated with production, storage and distribution of this fuel. Methanol, as a liquid fuel, can be the solution to these problems, although it presents some problems of toxicity and the performance of methanol fuel cells is lower than that of hydrogen fuel cells.

Methanol can be steam reformed to CO_2 and H_2; at the same time, some of the methanol decomposes to CO and H_2. The reforming reaction can be described by a first order kinetic equation r_1 (in relation to the methanol concentration) and the decomposition one by a zero order reaction rate r_2 [39]. According to Rabou [40], the problem can be treated analytically by taking the methanol conversion ratio as the variable of interest, and expressing the first order kinetic equation as a function of the conversion ratio (through the dependence of the methanol concentration on its conversion ratio). The needed catalyst weight for a given methanol flow and conversion fraction can be calculated as a function of temperature and pressure (Eq. (8)):

$$W = F\left[\left(\frac{U_s}{Z_s} + \frac{2Y_s}{Z_s^2}\right)\ln\left(\frac{Y_s}{Y_s - x_{met}Z_s}\right) - \frac{2x_{met}}{Z_s}\right] \quad (8)$$

The equation can also be inverted to calculate the methanol feed-flow rate necessary for a determined catalyst weight and a given conversion fraction.

Direct methanol fuel cells (DMFCs) are attractive for several applications. The structure of a single DMFC is an assembly of two porous electrodes on either side of a proton exchange membrane. Nowadays, a significant performance has been achieved by using an anodic catalyst based on Pt-Ru, while for the oxygen cathode the more important catalyst is Pt.

Jeng and Chen [41] present a mathematical model only for the anode of a DMFC. This model accounts for the mass transport in the flow channel (methanol transport, from the feed stream to the diffusion layer, due to the concentration gradient), transport in the diffusion layer (water transport and methanol transport by diffusion and convection), transport in the catalyst layer with a finite thickness (transport similar to that in the diffusion layer) and transport in the membrane (water transport, by diffusion and electro-osmotic drag, and methanol transport in a similar way as in the diffusion layer). The electrochemical reaction rate in the catalyst layer could be described by using a kinetic Tafel expression. In Nordlund and Lindbergh [42], an agglomerate model (in which each agglomerate is modeled as a sphere with a content of ionomer and catalyst on a carbon carrier) is used and kinetic equations based on a reaction mechanism (Eq. (9)) are derived

for methanol oxidation in the anode of a DMFC (adsorption steps coupled with Tafel kinetics). In fact, the kinetic model represents a simplified mechanism derived from a more complex one (Hamnett [43]):

$$\begin{aligned} &CH_3OH \underset{k_1'}{\overset{k_1}{\leftrightarrow}} CH_3OH_{ads} \\ &CH_3OH_{ads} \xrightarrow{k_2} CO_{ads} + 4H^+ + 4e^- \\ &H_2O \underset{k_3'}{\overset{k_3}{\leftrightarrow}} OH_{ads} + H^+ + e^- \\ &CO_{ads} + OH_{ads} \xrightarrow{k_4} CO_2 + H^+ + e^- \end{aligned} \quad (9)$$

Since heat is easily transported in a liquid fuel, temperature gradients are small and, therefore, considered negligible. Simulations showed that mass-transport limitations within the agglomerates are small and the model can be simplified (concentration gradients within the agglomerates can be neglected).

In Birgersson et al. [44], a one-phase model for mass, momentum and species transport in the anode of a DMFC is considered. The equations and boundary conditions were non-dimensionalized, and by recognizing that the ratio of the heights of the flow channel, porous backing and active catalyst layer to the anode length is much smaller than one (i.e., $h_f/L \ll 1$, $h_p/L \ll 1$ and $h_a \ll 1$), a reduced model was derived. The reduced model requires less computing time, a factor that makes it suitable for inclusion in studies where computational time may be a central matter. Besides, the study of the effect of design and operating parameters on the system behavior can be based on some of the non-dimensional parameters that arise from the analysis.

In Scott et al. [45], a DMFC model is reported, which accounts for the influence of methanol mass transport and of the CO_2 flow on the performance of the fuel cell. The model considers the hydrodynamics in the flow channels associated with the production of CO_2 and methanol mass transport in the diffusion electrode and the polymer membrane. The model also incorporates a semi-empirical equation for the open circuit potential in the presence of methanol crossover (in practice, a model of the effect of methanol on the mixed potential is required). Experimental data are used for validation. Mass transport at the anode is a factor that may limit the performance of the fuel cell.

In Sundmacher et al. [46], a mathematical model was developed to describe and analyze the behavior of a DMFC. The main phenomena are: convective mass transport in the anode compartment; methanol oxidation in the anode catalyst layer; oxygen reduction in the cathode catalyst layer; methanol and CO_2 mass transfer through the anode diffusion layer; methanol crossover and undesired methanol oxidation at the cathode catalyst layer as a result of methanol crossover. A multi-step reaction mechanism (Eq. (10), in which the methanol dissociative chemisorption was assumed to be the slow-step) was used to describe the electrochemical methanol

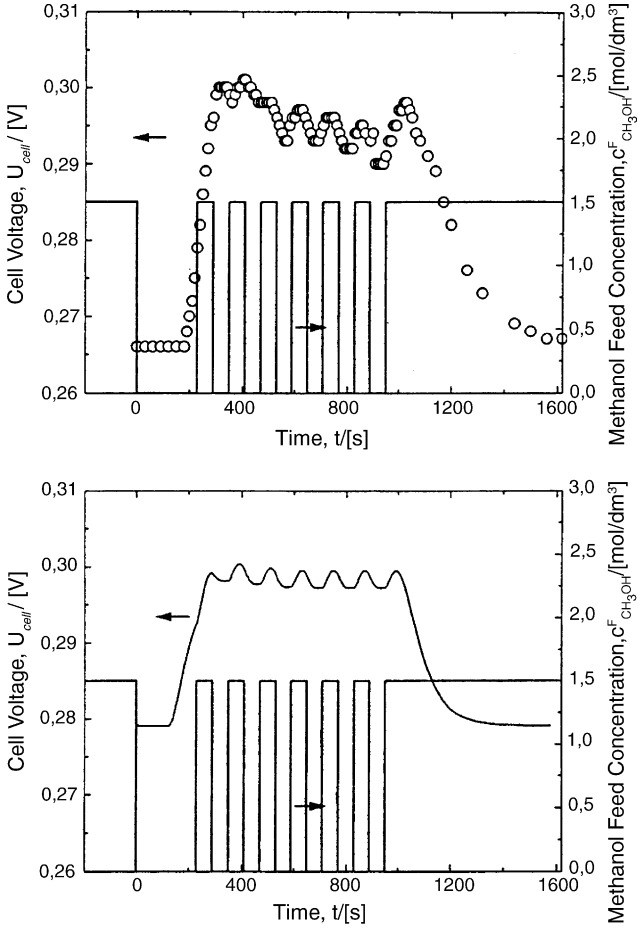

Fig. 10. Cell voltage response to periodically pulsed methanol feed concentrations: experimental data (top) and simulated data (bottom) (reprinted from [46], Copyright 2001, with permission from Elsevier Science).

oxidation at the Pt-Ru catalyst:

$$\begin{aligned} &3Pt + CH_3OH \leftrightarrow Pt_3 - COH + 3H^+ + 3e^- \\ &3Ru + 3H_2O \leftrightarrow 3Ru - OH + 3H^+ + 3e^- \\ &Pt_3 - COH + 2Ru - OH \leftrightarrow Pt - COOH + H_2O + 2Pt + 2Ru \\ &Pt - COOH + Ru - OH \leftrightarrow CO_2 + H_2O + Pt + Ru \end{aligned} \quad (10)$$

The mixtures at the anode were treated as a pure liquid phase mixture. To complete the model, mass balances for the anode compartment and the anode catalyst layer, and charge balances for the anode and cathode catalyst layers were formulated. The model of the effect of methanol oxidation at the cathode considers a parasitic current proportional to the methanol transport through the membrane (instantaneous methanol oxidation at the cathode). Experimentally, the authors observed that the cell voltage response to dynamic feeding showed a significant voltage increase after a sudden decrease in the methanol concentration in the feed. By simulation studies (Fig. 10), it was possible to verify that methanol crossover can be reduced by periodically pulsing

the methanol feed concentration, resulting in an increased cathode potential (and an increased cell voltage).

The authors affirm that some further model sophistications are necessary, such as considering CO_2 bubble formation in the anode.

In Meyers and Newman [47–49], a series of papers regarding the simulation of a DMFC is presented. Modeling of transport and kinetic phenomena is considered. The model describes the multi-component transport of species in the membrane by taking into account a thermodynamic framework developed in the first paper of the series [47]. The framework provides a means to quantify, in the second paper [48], the gradients in electrochemical potential (for hydrogen ions, for example, $\mu_{H^+} = R_g T \ln m_{H^+} + z_{H^+} F\phi$) for species in the membrane when describing the driving forces for the multi-component transport. Besides, a kinetic model (considering reaction steps very similar to those presented in Nordlund and Lindbergh [42]) is developed to describe methanol oxidation on the catalysts [48]. In the third paper of the series [49], the mathematical model is used to simulate the direct methanol fuel cell and quantify general aspects of its design.

In Argyropoulos et al. [50], a semi-empirical model based on Tafel-like kinetics for the methanol oxidation and oxygen reduction reactions and on effective mass transport coefficients is presented, which predicts the cell potential versus current density (Eq. (11)):

$$E_{cell} = E_0^* - b_{cell} \log I - RI + C_1 \ln(1 - C_2 I) \quad (11)$$

In Divisek et al. [51], a two-dimensional model of a DMFC was developed and tested. The model considers a calculation domain divided into different zones, with the diffusion layers as water–gas systems. The authors assume that the transport of water follows a standard two-phase flow mechanism. This can be seen as a generalized Darcy's law. The pore model for the transport of gases describes the interactions between the gases and their interactions with the pore walls, incorporated into the two-phase flow modeling approach. Regarding the dissolved species, a standard transport model is considered. For charged species, the appropriate potential equations are used. Energy considerations are derived from the Fourier law, with convection caused by the flow of fluids and gases. The reaction models account for the methanol (according to Kauranen et al. [52]) and oxygen kinetics. Condensation and evaporation processes are considered. The final equations are discretized in time and space with the objective of numerically solving the problem.

In Wang and Wang [53], two-phase modeling is considered (such as in Wang et al. [22]) in the cathode and in the anode (due to CO_2 evolution) of a DMFC. Tafel kinetic equations are considered to describe the oxygen reduction and methanol oxidation reactions (if necessary, adsorption steps may be included to describe methanol oxidation). The model also takes into account the mixed potential effect of methanol oxidation at the cathode as a result of methanol crossover. Simulation results showed (Fig. 11) that operating with small methanol feed concentrations suffers from low limiting current densities. In the medium current density range, an increase in methanol feed concentration led to a small decrease in cell voltage for methanol concentrations below 1 M. For a feed concentration larger than 2 M, the cell voltage was greatly reduced by excessive methanol crossover and the maximum current density was limited by the oxygen depletion at the cathode (resulting from excessive parasitic oxygen consumption).

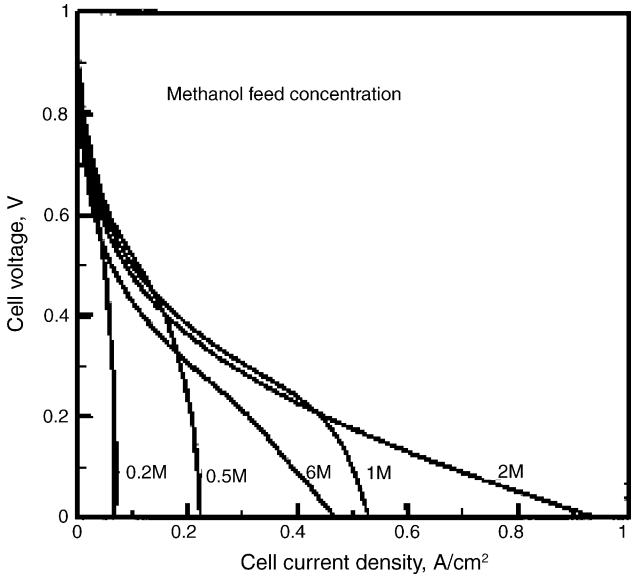

Fig. 11. Polarization curves with different methanol feed concentrations (reprinted from [53], Copyright 2003, reproduced by permission of The Electrochemical Society, Inc.).

Additional references regarding modeling of methanol fuel cells are: Baxter et al. [54] (in which kinetic and transport limitations are studied); Kulikovsky [55] (in which some local features due to geometric aspects, e.g. the low concentrations of reactants in front of current collectors, and mechanisms of methanol transport are studied); Fan et al. [56] (in which some local features generated by geometric aspects are also studied); Murgia et al. [57] (in which the effects of varying some empirical parameters are examined). Some works consider a vapor feed DMFC, such as Scott et al. [58] (in which methanol permeation through the polymer membrane and the caused mixed potential are studied); Dohle et al. [59] (in which the impact of methanol permeation through the electrolyte membrane is also considered); Kulikovsky et al. [60] (in which a new type of current collector, inside the backing and catalyst layers, which does not produce shaded regions in the catalyst layers, is considered).

Although discussing modeling of polymer electrolyte membrane fuel cell stacks is beyond the scope of this paper, we would like to point out the papers of Baschuk and Li [61], Hamelin et al. [62], Jiang and Chu [63], Lee and Lalk [64], Thirumalai and White [65] and Amphlett et al. [66]. Concerning the modeling of methanol fuel cell stacks, important

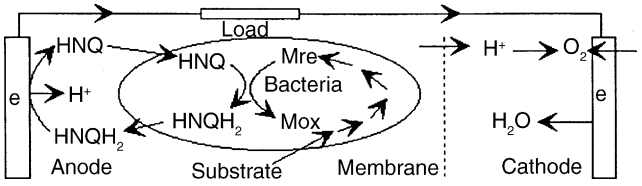

Fig. 12. Reaction diagram of the microbial fuel cell (reprinted from [73], Copyright 1995, with kind permission of Springer Science and Business Media).

references are Argyropoulos et al. [67–69], Scott et al. [70] and Simoglou et al. [71].

Considering briefly related types of fuel cells, the possibility of extracting electricity from low cost and abundant fuels by using either living microorganisms or their isolated enzymes, in biochemical fuel cells, is a fascinating point.

In a microbial fuel cell, the direct conversion of biochemical energy into electricity is accomplished. Basically, microbial fuel cells are divided into three types [72]: the first one involves the direct use of electroactive metabolites, such as hydrogen, produced by microbial metabolism from the substrate; the second type involves the use of mediators for electron transport from a certain metabolic pathway to electrodes (direct contact with the electrode surface is not required); the third one involves the use of microorganisms that may grow as a biofilm on the electrode surface (mediators are not necessary). When only enzymes instead of living microorganisms are used, in vitro systems are characterized.

In Zhang and Halme [73], a bacterial fuel cell consisting of a fuel cell device and a bioreactor is considered (Fig. 12).

The mediator used was a proper quinone. In a microbial fuel cell, besides the biochemical processes themselves, there are electrochemical and mass transport processes. In Zhang and Halme [73], the biochemical processes included a series of enzymatic reactions that could be modeled by Monod-like equations. Redox reactions were considered as first order processes. All mass transport processes were assumed to be fast enough when compared to biochemical and redox reactions. The process could be described by considering the proper differential equations and relationships, such as the Tafel equation for the activation overpotential. The simulation studies illustrated how the current output depends on the main system variables. The effect of initial substrate concentration, for example, is time delayed. A suitable mediator concentration can also be determined.

3. Conclusions

Modeling has allowed detailed studies concerning the development of polymer electrolyte membrane fuel cells, e.g. in discussing the electrocatalysis of the reactions and for the design of water-management schemes to cope with membrane dehydration. Results show that for cells operating with some membranes, water transport through the membrane is a limiting effect; for others, oxygen diffusion effects (in the gas diffusion electrode) may influence the potential–current relationship. In the presence of hydrogen dilution in the fuel stream, hydrogen is depleted at the reaction surface, resulting in substantial anode mass transport polarization (which can be of interest when considering reformed gas as the anode feed). Two-dimensional models have been used to represent reality, but three-dimensional models can cope with some (important) additional aspects. Consideration of two-phase transport in the air cathode of a proton exchange membrane fuel cell seems to be very appropriate (considering a non-isothermal model may improve the analysis); the inclusion of liquid water formation and transport can improve the predictive capability of the model. Knudsen diffusion has been neglected in the majority of the papers.

Regarding direct methanol fuel cells, mass transport is a factor that may limit the performance of the cell. Adsorption theory may be coupled to Tafel kinetics to describe methanol oxidation. Methanol crossover must also be taken into account (which can be reduced by periodically pulsing the methanol feed concentration). Extending the two-phase approach to the DMFC modeling is a recent, important point. Two-phase modeling may be considered both in the cathode and in the anode of a DMFC.

Regarding other types of fuel cells that may also operate with a polymer electrolyte, the possibility of extracting electricity from low cost and abundant fuels by using living microorganisms, in biochemical fuel cells, is a fascinating point. In contrast to the increasing experimental approaches, few authors have reported simulation studies of this kind of system. The study of biochemical fuel cells by applying proper modeling techniques (coupled to experimental studies) can help developments in this area, and certainly should be more explored in the future.

Acknowledgement

The authors thank FAPESP for the financial support.

References

[1] K. Haraldsson, K. Wipke, Evaluating PEM fuel cell system models, J. Power Sources 126 (2004) 88–97.
[2] J.T. Wang, R.F. Savinell, Simulation studies on the fuel electrode of a H_2–O_2 polymer electrolyte fuel cell, Electrochim. Acta 37 (1992) 2737–2745.
[3] J. Kim, S.M. Lee, S. Srinivasan, Modeling of proton exchange membrane fuel cell performance with an empirical equation, J. Electrochem. Soc. 142 (1995) 2670–2674.
[4] G. Squadrito, G. Maggio, E. Passalacqua, F. Lufrano, A. Patti, An empirical equation for polymer electrolyte fuel cell (PEFC) behavior, J. Appl. Electrochem. 29 (1999) 1449–1455.
[5] T.E. Springer, I.D. Raistrick, Electrical impedance of a pore wall for the flooded-agglomerate model of porous gas-diffusion electrodes, J. Electrochem. Soc. 136 (1989) 1594–1603.
[6] J. Giner, C. Hunter, Mechanism of operation of teflon-bonded gas diffusion electrode–a mathematical model, J. Electrochem. Soc. 116 (1969) 1124–1130.

[7] J. Perez, E.R. Gonzalez, E.A. Ticianelli, Oxygen electrocatalysis on thin porous coating rotating platinum electrodes, Electrochim. Acta 44 (1998) 1329–1339.
[8] T.E. Springer, T.A. Zawodzinski, S. Gottesfeld, Polymer electrolyte fuel cell model, J. Electrochem. Soc. 138 (1991) 2334–2342.
[9] D.M. Bernardi, M.W. Verbrugge, A mathematical model of the solid-polymer-electrolyte fuel cell, J. Electrochem. Soc. 139 (1992) 2477–2491.
[10] T.F. Fuller, J. Newman, Water and thermal management in solid-polymer-electrolyte fuel cells, J. Electrochem. Soc. 140 (1993) 1218–1225.
[11] T.V. Nguyen, R.E. White, A water and heat management model for proton-exchange-membrane fuel cells, J. Electrochem. Soc. 140 (1993) 2178–2186.
[12] J.S. Yi, T.V. Nguyen, An along-the-channel model for proton exchange membrane fuel cells, J. Electrochem. Soc. 145 (1998) 1149–1159.
[13] A. De Souza, E.R. Gonzalez, Influence of the operational parameters on the performance of polymer electrolyte membrane fuel cells with different flow fields, J. Solid State Electrochem. 7 (2003) 651–657.
[14] K. Dannenberg, P. Ekdunge, G. Lindbergh, Mathematical model of the PEMFC, J. Appl. Electrochem. 30 (2000) 1377–1387.
[15] D.R. Sena, E.A. Ticianelli, V.A. Paganin, E.R. Gonzalez, Effect of water transport in a PEFC at low temperatures operating with dry hydrogen, J. Electroanal. Chem. 477 (1999) 164–170.
[16] V. Gurau, H. Liu, S. Kakaç, Two-dimensional model for proton exchange membrane fuel cells, AIChE J. 44 (1998) 2410–2422.
[17] S. Um, C.Y. Wang, K.S. Chen, Computational fluid dynamics modeling of proton exchange membrane fuel cells, J. Electrochem. Soc. 147 (2000) 4485–4493.
[18] S. Um, C.Y. Wang, Three-dimensional analysis of transport and electrochemical reactions in polymer electrolyte fuel cells, J. Power Sources 125 (2004) 40–51.
[19] J.S. Yi, T.V. Nguyen, Multicomponent transport in porous electrodes of proton exchange membrane fuel cells using the interdigitated gas distributors, J. Electrochem. Soc. 146 (1999) 38–45.
[20] S. Dutta, S. Shimpalee, J. Van Zee, Numerical prediction of mass-exchange between cathode and anode channels in a PEM fuel cell, Int. J. Heat Mass Transfer 44 (2001) 2029–2042.
[21] G.J.M. Janssen, A Phenomenological model of water transport in a proton exchange membrane fuel cell, J. Electrochem. Soc. 148 (2001) A1313–A1323.
[22] Z.H. Wang, C.Y. Wang, K.S. Chen, Two-phase flow and transport in the air cathode of proton exchange membrane fuel cells, J. Power Sources 94 (2001) 40–50.
[23] C.Y. Wang, P. Cheng, A multiphase mixture model for multiphase, multicomponent transport in capillary porous media. 1, Int. J. Heat Mass Transfer 39 (1996) 3607–3618.
[24] P. Cheng, C.Y. Wang, A Multiphase mixture model for multiphase, multicomponent transport in capillary porous media. 2, Int. J. Heat Mass Transfer 39 (1996) 3619–3632.
[25] T. Berning, D.M. Lu, N. Djilali, Three-dimensional computational analysis of transport phenomena in a PEM fuel cell, J. Power Sources 106 (2002) 284–294.
[26] L. Pisani, G. Murgia, M. Valentini, B. D'Aguanno, A new semi-empirical approach to performance curves of polymer electrolyte fuel cells, J. Power Sources 108 (2002) 192–203.
[27] S. Mazumder, J.V. Cole, Rigorous 3-D mathematical modeling of PEM fuel cells—I, J. Electrochem. Soc. 150 (2003) A1503–A1509.
[28] S. Mazumder, J.V. Cole, Rigorous 3-D mathematical modeling of PEM fuel cells—II, J. Electrochem. Soc. 150 (2003) A1510–A1517.
[29] E.A. Ticianelli, C.R. Derouin, S. Srinivasan, Localization of platinum in low catalyst loading electrodes to attain high-power densities in SPE fuel-cells, J. Electroanal. Chem. 251 (1988) 275–295.
[30] E.A. Ticianelli, C.R. Derouin, A. Redondo, S. Srinivasan, Methods to advance technology of proton-exchange membrane fuel-cells, J. Electrochem. Soc. 135 (1988) 2209–2214.
[31] M. Wöhr, K. Bolwin, W. Schnurnberger, M. Fisher, W. Neubrand, G. Eigenberger, Dynamic modelling and simulation of a polymer membrane fuel cell including mass transport limitation, Int. J. Hydrogen Energy 23 (1998) 213–218.
[32] M. Eikerling, A.A. Kornyshev, Modeling the performance of the cathode catalyst layer of polymer electrolyte fuel cells, J. Electroanal. Chem. 453 (1998) 89–106.
[33] A.A. Kulikovsky, J. Divisek, A.A. Kornyshev, Modeling the cathode compartment of polymer electrolyte fuel cells: dead and active reaction zones, J. Electrochem. Soc. 146 (1999) 3981–3991.
[34] R.F. Mann, J.C. Amphlett, M.A.I. Hooper, H.M. Jensen, B.A. Peppley, P.R. Roberge, Development and application of a generalized steady-state electrochemical Model for a PEM fuel cell, J. Power Sources 86 (2000) 173–180.
[35] G. Maggio, V. Recupero, L. Pino, Modeling polymer electrolyte fuel cells: an innovative approach, J. Power Sources 101 (2001) 275–286.
[36] A. Rowe, X. Li, Mathematical modeling of proton exchange membrane fuel cells, J. Power Sources 102 (2001) 82–96.
[37] S.H. Ge, B.L. Yi, A mathematical model for PEMFC in different flow modes, J. Power Sources 124 (2003) 1–11.
[38] S. Yerramalla, A. Davari, A. Feliachi, T. Biswas, Modeling and simulation of a polymer electrolyte membrane fuel cell, J. Power Sources 124 (2003) 104–113.
[39] J.C. Amphlett, K.A.M. Creber, J.M. Davis, R.F. Mann, B.A. Peppley, D.M. Stokes, Hydrogen production by steam reforming of methanol for polymer electrolyte fuel-cells, Int. J. Hydrogen Energy 19 (1994) 131–137.
[40] L.P.L.M. Rabou, Modeling of a variable-flow methanol reformer for a polymer electrolyte fuel cell, Int. J. Hydrogen Energy 20 (1995) 845–848.
[41] K.T. Jeng, C.W. Chen, Modeling and simulation of a direct methanol fuel cell anode, J. Power Sources 112 (2002) 367–375.
[42] J. Norlund, G. Lindbergh, A model for the porous direct methanol fuel cell, J. Electrochem. Soc. 149 (2002) A1107–A1113.
[43] A. Hamnett, Mechanism and electrocatalysis in the direct methanol fuel cell, Catal. Today 38 (1997) 445–457.
[44] E. Birgersson, J. Nordlund, H. Ekström, M. Vynnicky, G. Lindbergh, Reduced Two-dimensional one-phase model for analysis of the anode of a DMFC, J. Electrochem. Soc. 150 (2003) A1368–A1376.
[45] K. Scott, P. Argyropoulos, K. Sundmacher, A model for the liquid feed direct methanol fuel cell, J. Electroanal. Chem. 477 (1999) 97–110.
[46] K. Sundmacher, T. Schultz, S. Zhou, K. Scott, M. Ginkel, E.D. Gilles, Dynamics of the direct methanol fuel cell (DMFC): experiments and model based analysis, Chem. Eng. Sci. 56 (2001) 333–341.
[47] J.P. Meyers, J. Newman, Simulation of the direct methanol fuel cell. I, J. Electrochem. Soc. 149 (2002) A710–A717.
[48] J.P. Meyers, J. Newman, Simulation of the direct methanol fuel cell. II, J. Electrochem. Soc. 149 (2002) A718–A728.
[49] J.P. Meyers, J. Newman, Simulation of the direct methanol fuel cell. III, J. Electrochem. Soc. 149 (2002) A729–A735.
[50] P. Argyropoulos, K. Scott, A.K. Shukla, C. Jackson, A semi-empirical model of the direct methanol fuel cell performance. Part I, J. Power Sources 123 (2003) 190–199.
[51] J. Divisek, J. Fuhrmann, K. Gärtner, R. Jung, Performance modeling of a direct methanol fuel cell, J. Electrochem. Soc. 150 (2003) A811–A825.
[52] P.S. Kauranen, E. Skou, J. Munk, Kinetics of methanol oxidation on carbon-suported Pt and Pt-Ru Catalysts, J. Electroanal. Chem. 404 (1996) 1–13.
[53] Z.H. Wang, C.Y. Wang, Mathematical modeling of liquid-feed direct methanol fuel cells, J. Electrochem. Soc. 150 (2003) A508–A519.
[54] S.F. Baxter, V.S. Battaglia, R.E. White, Methanol fuel cell model: anode, J. Electrochem. Soc. 146 (1999) 437–447.
[55] A.A. Kulikovsky, Two-dimensional numerical modelling of a direct methanol fuel cell, J. Appl. Electrochem. 30 (2000) 1005–1014.

[56] J.R. Fan, G.L. Hu, J. Yao, K.F. Cen, A two-dimensional mathematical model of liquid-feed direct methanol fuel cells, Energy Fuels 16 (2002) 1591–1598.
[57] G. Murgia, L. Pisani, A.K. Shukla, K. Scott, A numerical model of a liquid-feed solid polymer electrolyte DMFC and its experimental validation, J. Electrochem. Soc. 150 (2003) A1231–A1245.
[58] K. Scott, W. Taama, J. Cruikshank, Performance of a direct methanol fuel cell, J. Appl. Electrochem. 28 (1998) 289–297.
[59] H. Dohle, J. Divisek, R. Jung, Process engineering of the direct methanol fuel cell, J. Power Sources 86 (2000) 469–477.
[60] A.A. Kulikovsky, J. Divisek, A.A. Kornyshev, Two-dimensional simulation of direct methanol fuel cell—a new (embedded) type of current collector, J. Electrochem. Soc. 147 (2000) 953–959.
[61] J.J. Baschuk, X.G. Li, Modeling of polymer electrolyte membrane fuel cell stacks based on a hydraulic network approach, Int. J. Energy Res. 28 (2004) 697–724.
[62] J. Hamelin, K. Agbossou, A. Laperriere, F. Laurencelle, T.K. Bose, Dynamic behavior of a PEM fuel cell stack for stationary applications, Int. J. Hydrogen Energy 26 (2001) 625–629.
[63] R.Z. Jiang, D. Chu, Voltage-time behavior of a polymer electrolyte membrane fuel cell stack at constant current discharge, J. Power Sources 92 (2001) 193–198.
[64] J.H. Lee, T.R. Lalk, Modeling fuel cell stack systems, J. Power Sources 73 (1998) 229–241.
[65] D. Thirumalai, R.E. White, Mathematical modeling of proton-exchange-membrane fuel-cell stacks, J. Electrochem. Soc. 144 (1997) 1717–1723.
[66] J.C. Amphlett, R.M. Baumert, R.F. Mann, B.A. Peppley, P.R. Roberge, A. Rodrigues, Parametric modeling of the performance of a 5-kW proton-exchange membrane fuel-cell stack, J. Power Sources 49 (1994) 349–356.
[67] P. Argyropoulos, K. Scott, W.M. Taama, One-dimensional thermal model for direct methanol fuel cell stacks—Part I, J. Power Sources 79 (1999) 169–183.
[68] P. Argyropoulos, K. Scott, W.M. Taama, Hydrodynamic modelling of direct methanol liquid feed fuel cell stacks, J. Appl. Electrochem. 30 (2000) 899–913.
[69] P. Argyropoulos, K. Scott, W.M. Taama, Modeling flow distribution for internally manifold direct methanol fuel cell stacks, Chem. Eng. Technol. 23 (2000) 985–995.
[70] K. Scott, P. Argyropoulos, W.M. Taama, Modeling transport phenomena and performance of direct methanol fuel cell stacks, Chem. Eng. Res. Des. 78 (2000) 881–888.
[71] A. Simoglou, P. Argyropoulos, E.B. Martin, K. Scott, A.J. Morris, W.M. Taama, Dynamic modelling of the voltage response of direct methanol fuel cells and stacks. Part I, Chem. Eng. Sci. 56 (2001) 6761–6772.
[72] L.T. Angenent, K. Karim, M.H. Al-Dahhan, B.A. Wrenn, R. Domíguez-Espinosa, Production of bioenergy and biochemicals from industrial and agricultural wastewater, Trends Biotechnol. 22 (2004) 477–485.
[73] X.C. Zhang, A. Halme, Modeling of a microbial fuel cell process, Biotechnol. Lett. 17 (1995) 809–814.